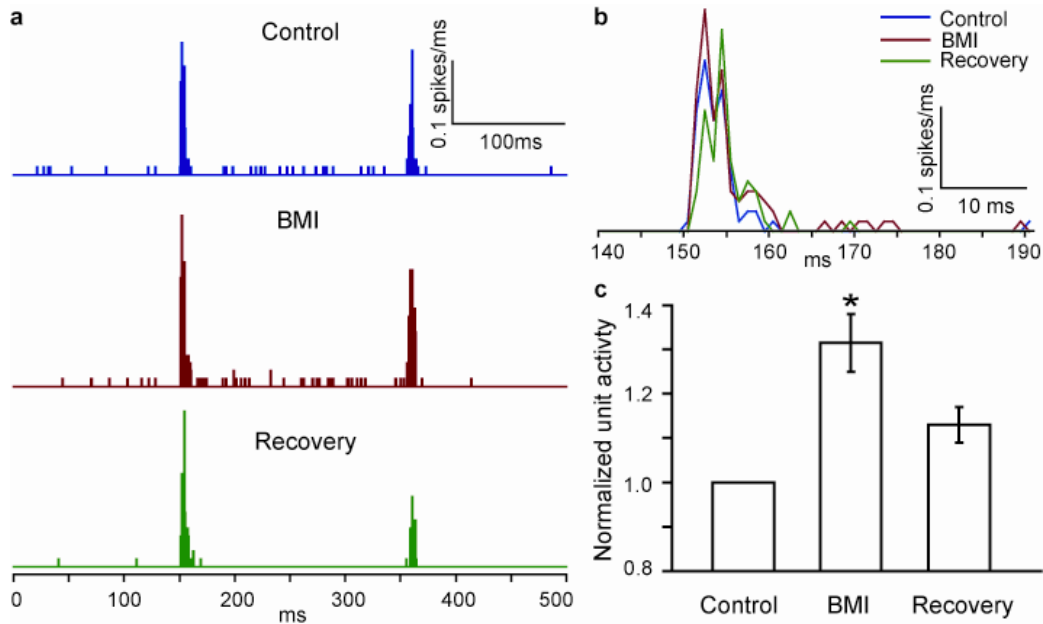# Motor Modulation of Afferent Somatosensory Circuits

SooHyun Lee, George E. Carvell, and Daniel J. Simons

Supplementary Figure 1. Reversible effect on S1 neurons of BMI application to vFMCx. (**a** and **b**) PSTHs of an example layer 6 (L-6) neuron in S1. Activity is shown for the total duration of the trial (**a**) and at an expanded time scale comprising the response to the onset of principal whisker deflection (**b**). Microiontophoretic application of 10 mM BMI for 5 min causes 1.3-fold increase in unit activity relative to the control level (Control 0.83 ± 0.32 spikes stimulus^{-1}, BMI 1.10 ± 0.38, paired t-test, $p<0.05$). Activity returns to baseline within 40 min of cessation of BMI application (0.97-fold change). (**c**) Single unit activity of 21 L-6 neurons in S1 (n= 4 experiments) during BMI application and recovery to aligned vMFCx was normalized to unit activity during the control condition. During BMI application to vFMCx, evoked responses of S1 L-6 neurons are significantly increased (1.32-fold, paired t-test, * denotes $p = 0.01$). 30-60 min after termination of BMI vFMCx microiontophoresis, the S1 evoked responses recovered to control levels (1.13-fold, $p=0.8$). Error bars indicate mean $\pm$ s.e.m.

targeted whisker

terminal segments of wires
were stripped (<1mm)
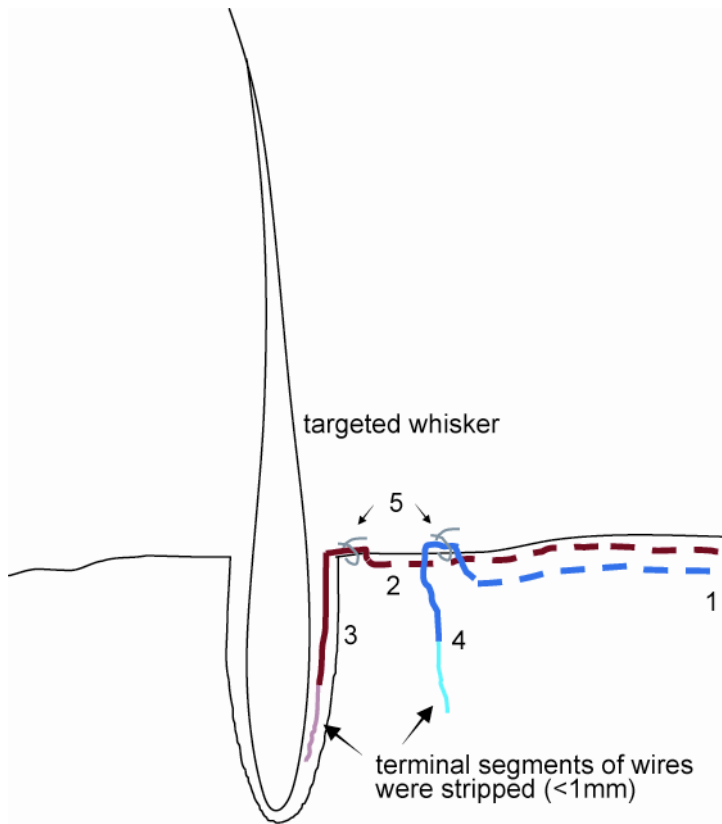
Supplementary Figure 2. Schematic diagram of implantation method of whisker follicle stimulating wires. 1. A pair of Teflon-coated stainless steel (0.003") wires, whose terminal 1 mm segments were stripped of insulation, was tunneled subcutaneously to the mystacial pad contralateral to the VPm recording site. 2. The wires were led out from the skin immediately adjacent to the targeted whisker corresponding physiologically to the site of implantation of the VPm recording electrode. 3. The stimulation wire was bent back on itself and inserted into the whisker follicle. 4. The other wire was inserted nearby into the skin to serve as the indifferent electrode. 5. Both wires were sutured to the skin.
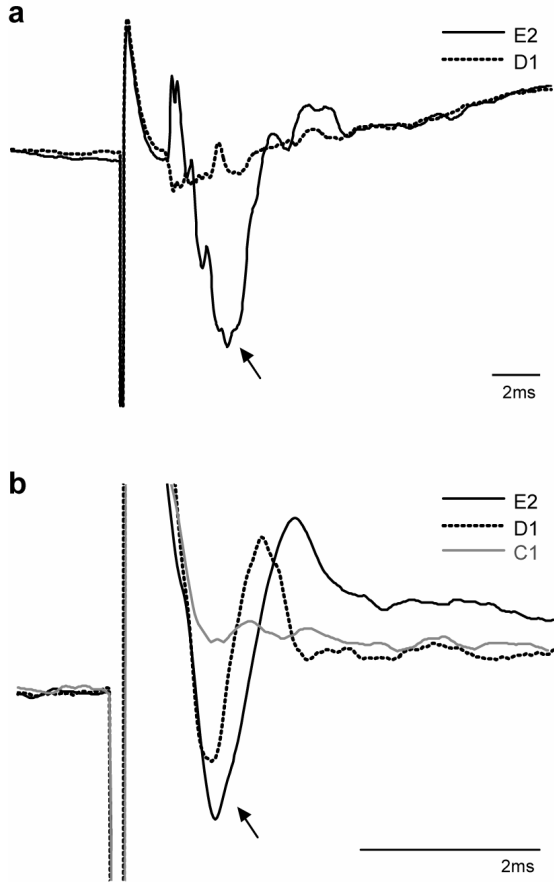
Supplementary Figure 3. Topographic specificity of whisker follicle (a) and medial lemniscal (b) stimulation. (**a**) E2 whisker follicle (WF) stimulation evoked a pronounced LFP negativity in the physiologically defined E2 thalamic barreloid but not in D1. (**b**) ML-evoked responses as a function of VPm recording sites. Data were obtained from a single anesthetized rat in each panel. Arrows indicate initial negativity of the response.
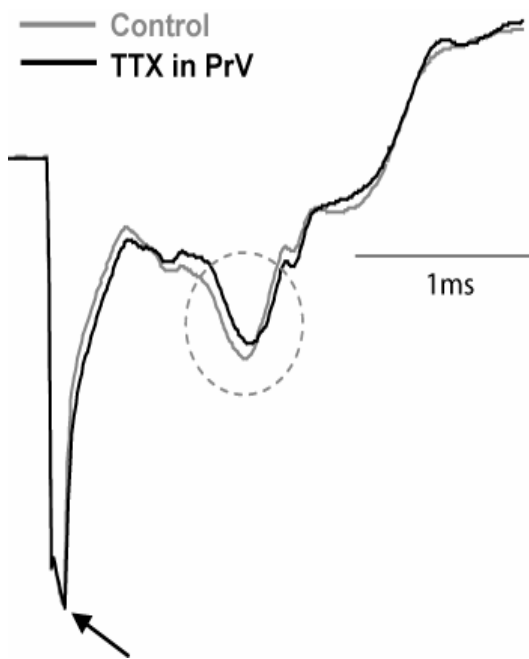
Supplementary Figure 4. ML-evoked VPm LFP is unaffected by TTX application to PrV. The late VPm response component (gray dashed ellipse) is intact during PrV inactivation; a brief early response component (arrow) is visible at the end of the stimulus artifact. Recording was obtained from an anesthetized rat.

ML stimulation evoked thalamic LFP: early and late components

Our ML stimulation parameters consistently elicited two negative peaks in the VPm LFP trace; an early and a late component. These two components had latencies of 0.59 ± 0.05 and 1.92 ± 0.10 ms, respectively. The early component likely represents the thalamic response directly evoked by electrical stimulation of presynaptic fibers. Three possible scenarios can explain the late component. One, the late component may reflect thalamic responses to firing of PrV neurons which are antidromically activated by back-propagating action potentials elicited by the ML electric shock. To test this possibility, in a control experiment we pharmacologically inactivated PrV using

tetrodotoxin (TTX), a Na$^+$ channel blocker. Inactivation of PrV neurons would abolish VPm responses evoked by antidromic spikes in PrV. We found that ML stimulation still induced the late component after PrV inactivation; thus, antidromically reflected PrV firing is not responsible for the late component. A second possibility is that the early thalamic response evoked by ML stimulation excites neurons in L-6, including corticothalamic cells. In this scenario, corticothalamic feedback would provide a second, longer-latency source of thalamic activation. However, there are at least two synapses plus two axon conduction times in this thalamo-cortico-thalamic circuit; the time difference between early and late components (1.3 ms) is therefore too short to be evoked via cortical feedback[1,2]. Lastly, direct electrical stimulation of presynaptic fibers in ML likely causes strong depolarization and robust spiking of VPm neurons. The second peak may thus reflect synchronous discharges of VPm neurons with the timing of the second peak determined by the neurons' refractory period of ~1.0-1.5 ms.
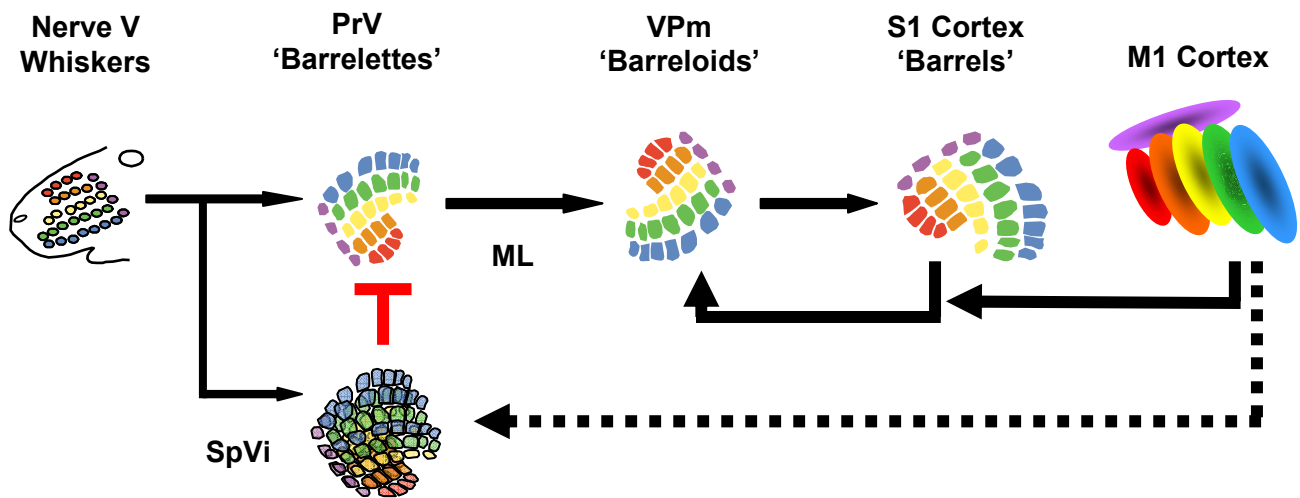
Supplementary Figure 5. Schematic diagram of a whisker-related sensorimotor circuit. Vibrissal/face primary motor cortex (M1) facilitates C-T neurons in topographically aligned barrel-related columns of S1. S1 C-T neurons project to the topographically corresponding barreloid where they in turn increase the excitability of VPm neurons. Simultaneously, motor cortex engages inhibitory neurons in SpVi that may globally suppress activity in PrV (red "T"), the main afferent relay to VPm via the trigeminothalamic tract, here denoted as the medial lemniscus (ML)[3]. The circuitry by which descending M1-related corticofugal signals cause SpVi to inhibit or "gate" activity in PrV is an active area of investigation[3] (indicated by dashed line). SpVi is shown with overlapping whisker representations indicating the predominance of large receptive fields there. See text for description of possible function during whisking behavior.
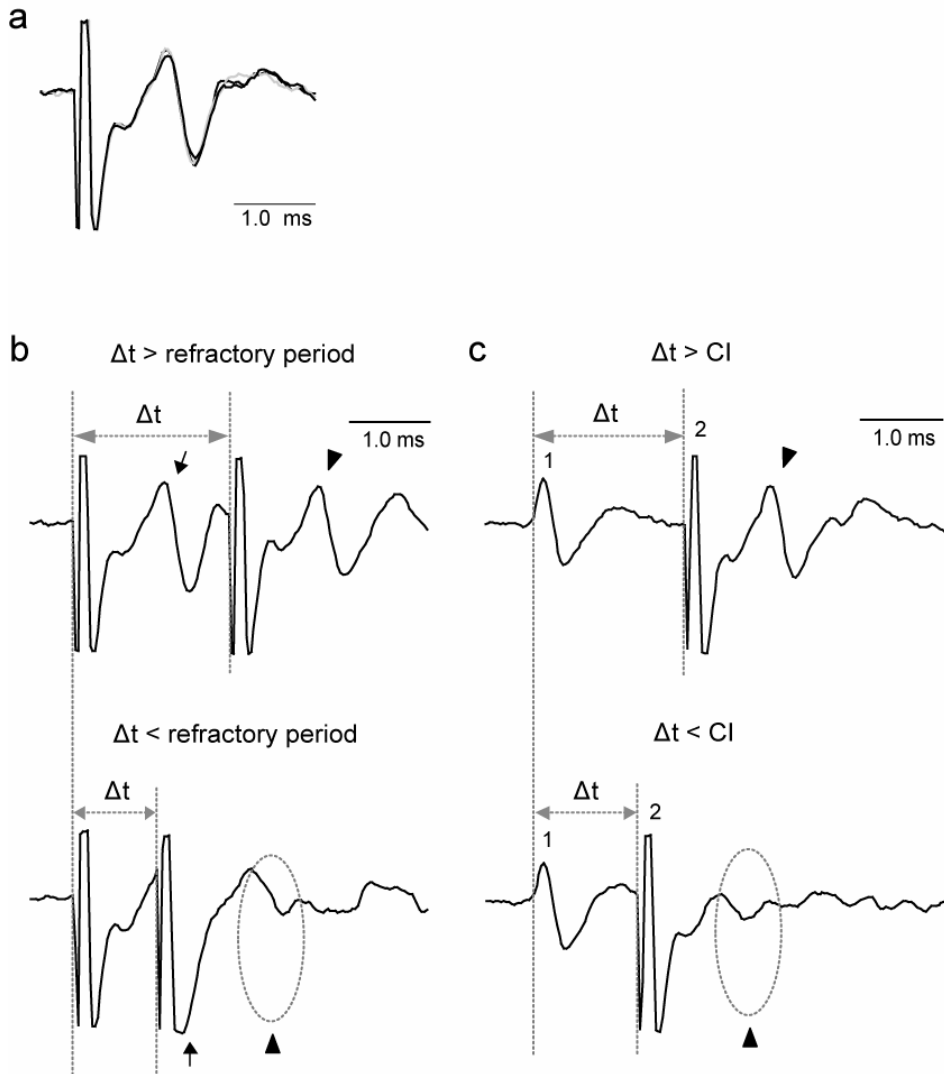
Supplementary Figure 6. Antidromic identification of C-T neurons. (**a**) Three superimposed traces of antidromic spikes demonstrating little variability in latency in response to electrical pulses delivered to a topographically aligned VPm site. (**b**) Measurement of refractory period using paired and temporally separated (Δt) electrical stimuli. In top trace, spikes indicated by the arrow and arrowhead are evoked by the first and second stimulus, respectively. Bottom trace: with short Δt, a second spike is no longer evoked at the expected time (ellipse). Arrow indicates expected time of occurrence of first spike which is partially obscured by the stimulus artifact. Vertical axis

at c and b are same in arbitrary unit. (**c**) Collision test verifying the antidromic activation

of the cell shown in **b**. A spontaneous spike (1) triggers the electrical stimulus (2), which

in turn evokes an antidromic spike (arrowhead). As Δt becomes smaller, the

spontaneous and antidromic spikes eventually collide. This interval is designated as the

collision interval (CI). CI is predicted to equal the sum of antidromic latency and the

refractory period. Top trace: Δt is longer than CI of the neuron, and the spike evoked by

the trigger stimulus does not collide with the spontaneous spike. Bottom trace: Δt is

shorter than CI, and the spontaneous and antidromic spikes collide. Note the absence

of the expected antidromic spike (arrowhead and ellipse).

a

b

Power spectral density

Frequency (Hz)
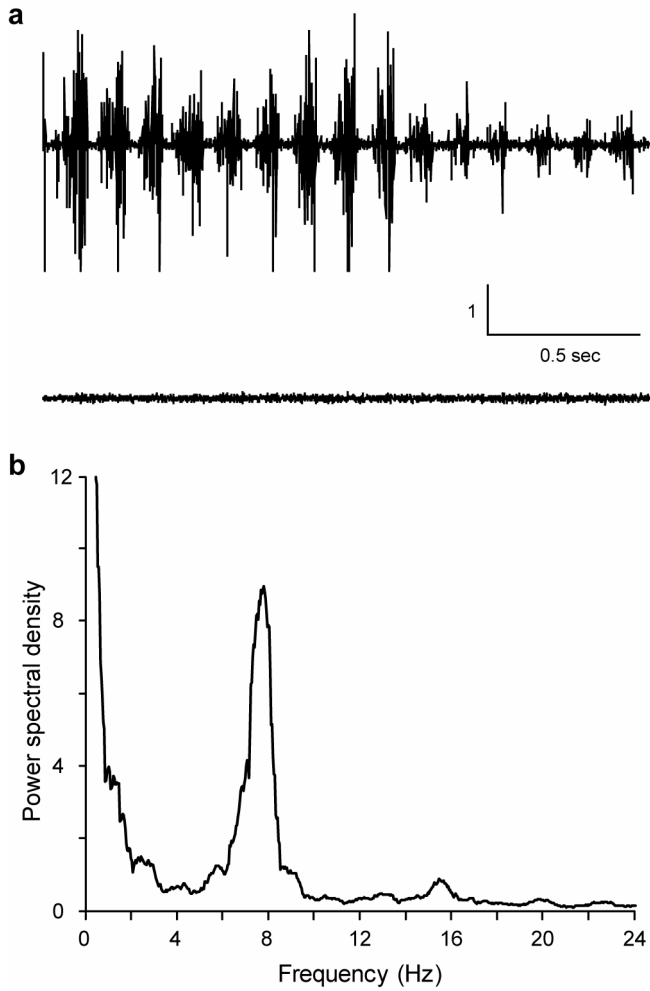
Supplementary Figure 7. EMG activity. (**a**) Example of EMG activity during whisking (top) and non-whisking (bottom) over a 2 sec period. (b) Power spectral density of rectified EMG from tope trace in a) showing a peak at 6-9 Hz.
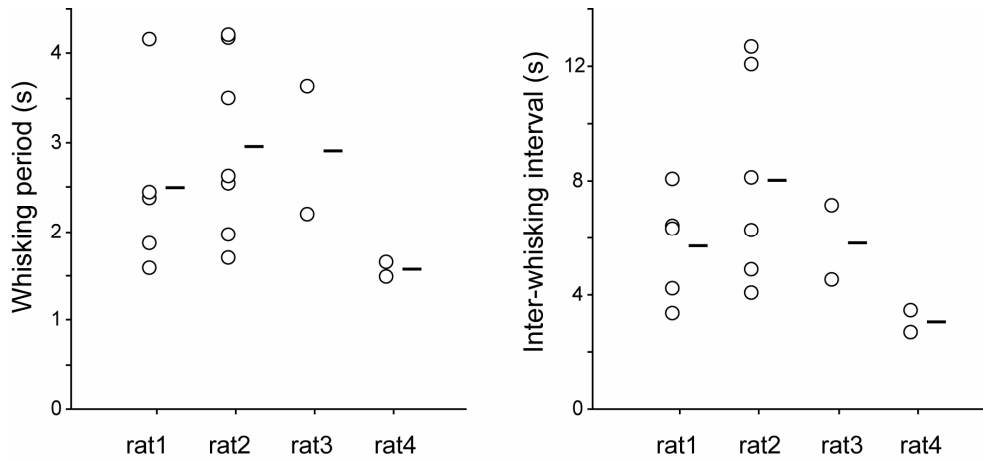
Supplementary Figure 8. Whisking periods (left) and inter-whisking intervals (right) from 4 animals. Averaged whisking period across animals is 2.63 ± 2.31 sec. Averaged inter-whisking interval is 6.38 ± 4.30 sec. Open circles indicates each recording day and black lines indicate means of each animal.

Supplementary Table 1. Axon conduction properties of CT neurons (n=38).

	Conduction velocity (m/s)	Supernormality (%)	Refractory period (ms)
Mean ± Std. Dev.	4.43 ± 0.86	9.21 ± 2.37	1.25 ± 0.22
Median	4.38	7.22	1.37

REFERENCES

1. Kyriazi, H.T. & Simons, D.J. Thalamocortical response transformations in simulated whisker barrels. *J. Neurosci.* **13**, 1601-15 (1993).

2. Kelly, M.K., Carvell, G.E., Hartings, J.A. & Simons, D.J. Axonal conduction properties of antidromically identified neurons in rat barrel cortex. *Somatosens. Mot. Res.* **18**, 202-10 (2001).

3. Furuta, T. *et al*. Inhibitory gating of vibrissal inputs in the brainstem. *J. Neurosci.* **28**, 1789-97 (2008).